**PAPER • OPEN ACCESS**

# Validation and comparison of aerodynamic modelling approaches for wind turbines

To cite this article: F. Blondel *et al* 2016 *J. Phys.: Conf. Ser.* **753** 022029

View the article online for updates and enhancements.

# Validation and comparison of aerodynamic modelling approaches for wind turbines

**F. Blondel**[1]**, R. Boisard**[2]**, M. Milekovic**[3]**, G. Ferrer**[1]**, C. Lienard**[2]**, D. Teixeira**[1]

[1] IFP Energies nouvelles, 1-4 avenue du Bois Préau, 92852 Rueil-Malmaison, France
[2] ONERA The French Aerospace Lab, F-92190 Meudon, France
[3] IFP Energies nouvelles, Rond-point de l'échangeur de Solaize, 69360 Solaize, France

E-mail: `frederic.blondel@ifpen.fr`

**Abstract.** The development of large capacity Floating Offshore Wind Turbines (FOWT) is an interdisciplinary challenge for the design solvers, requiring accurate modelling of both hydrodynamics, elasticity, servodynamics and aerodynamics all together. Floating platforms will induce low-frequency unsteadiness, and for large capacity turbines, the blade induced vibrations will lead to high-frequency unsteadiness. While yawed inflow conditions are still a challenge for commonly used aerodynamic methods such as the Blade Element Momentum method (BEM), the new sources of unsteadiness involved by large turbine scales and floater motions have to be tackled accurately, keeping the computational cost small enough to be compatible with design and certification purposes. In the light of this, this paper will focus on the comparison of three aerodynamic solvers based on BEM and vortex methods, on standard, yawed and unsteady inflow conditions. We will focus here on up-to-date wind tunnel experiments, such as the Unsteady Aerodynamics Experiment (UAE) database and the MexNext international project.

## 1. Introduction

Nowadays, most of the design software rely on the Blade Element Momentum models [10]. Those methods are based on strong hypotheses, partially overcame through analytical corrections, that introduce empiricism in the models. The reliability of the model is then questionable, especially in the framework of large fixed and floating offshore wind turbines, which tend to become larger and larger, reaching $10MW$ or more [2]. On the other side, more physical models, such as the vortex methods, that require less analytical corrections, are being increasingly used. The development of algorithms and new computational architectures have strongly reduced the computational time of vortex methods, which is crucial in the light of the large databases that have to be tackled for certification purposes. Vortex methods provide different solutions to model the wake, such as vortex points, filaments or panels. The aim of this paper is to compare a BEM solver and two vortex solvers designed to be coupled with the aero-servo-hydro-elastic solver DeepLines Wind$^{TM}$ [8] against up-to-date wind tunnels experiments, identify the cases on which BEM models are not accurate enough, and evaluate the potential of vortex models on those cases. The two lifting-line solvers are based on different wake models, a free-wake vortex filaments model and a free-wake vortex panel wake model. The impact of the wake model on the lifting-line results will be analysed.

## 2. Computational tools

### 2.1. AeroDeeP: BEM based aerodynamic library

AeroDeeP is based on a the widely used Glauert's Blade Element Momentum method [4], inspired from the Rankine-Froude theory, using two-dimensional airfoil characteristics to evaluate the forces at each blade element. Induction factors, which represent the momentum loss due to the presence of the rotor, are computed in both axial and tangential directions along the blade span. In order to overcome the major limitations of the classical BEM theory, corrections have been implemented to account for hub and tip losses, turbulent wake state, tower shadowing, dynamic inflow (i.e. unsteady BEM), dynamic stall, as well as skewed rotor configurations.

### 2.2. CASTOR: Lifting-Line / Free-Wake aerodynamic library

CASTOR (Code Aerodynamique pour la Simulation de Turbines OffshoRe) is a free-wake vortex filament lifting-line solver based on the generalized Prandtl lifting-line theory (see [14], [7]). Various flow effects such as turbulent wake state, dynamic inflow, hub and tip losses, as well as skewed rotor configurations are inherently taken into account. Similarly to the BEM method, CASTOR is based on airfoil polars, so that blade surfaces do not have to be modeled. In order to reduce the computational cost, CASTOR is based on an hybrid *OpenMP / GPU* implementation, thereby reducing the computational times up to two orders of magnitude when compared to sequential *CPU* implementations. The presence of the ground can be taken into account through the mirror technique, and the Beddoes-Leishman modified Risoe stall model [6] has been implemented. CASTOR will be referred to as Lifting-Line (Prandtl) in the following.

### 2.3. PUMA: Lifting-Line / Free-Wake aerodynamic library

The PUMA (Potential Unsteady Methods for Aerodynamics) code which is developed at ONERA since 2013 is based on a long lasting knowledge about free wake methods for helicopter aerodynamics. It is built on a coupling between a kinematic module and an aerodynamic module which relies on a free wake model combined to a lifting line approach. The free wake model is based on Mudry theory [9] which rigorously describes the unsteady evolution of a wake modeled by a potential discontinuity surface while the lifting line method relies on $2D$ airfoils characteristics and can handle some $3D$ corrections for blade sweep and $2D$ unsteady aerodynamics effects through dynamics stall models. In order to reduce computational time the code has been parallelized using OpenMP and the Multilevel Fast Multipole Method has been implemented for the computation of the velocities induced by each wake panel on any element. Thanks to the versatility offered by the modular approach of PUMA, we were able to directly plug the aerodynamic module to the Deeplines Wind$^{\text{TM}}$ solver, which provide the needed kinematic data in place of the built-in PUMA's module. PUMA will be referred to as Lifting-Line (Mudry) in the following.

### 2.4. Deeplines Wind $^{TM}$ and coupling strategy

DeepLines Wind$^{\text{TM}}$ [8] is an aero-servo-hydro-elastic solver developed by Principia/IFPEN that simulate loads and deformation of onshore, offshore and floating wind turbine in operation. It offers the possibility to be coupled with different aerodynamic libraries. The coupling with external solvers is realised through APIs (Application Programming Interface) designed to be as generic as possible. At each time step, information related to the wind turbine geometry and motions are sent to the aerodynamic solver, that sends back the aerodynamic loads on the blades. Those information are:

- Blade, tower and hub elements orientations;
- Blade, tower and hub elements position;
- Blade, tower and hub elements translation and rotation velocities and accelerations;

- Wind velocity at any positions specified by the aerodynamic solvers.

Based on this architecture, in-house (AeroDeeP, CASTOR) and external (PUMA) aerodynamic libraries have been coupled to the DeepLines Wind$^{TM}$ solver. For this specific study, in order to simplify the comparison between the different aerodynamics models, the libraries were coupled with a simple kinetic module, based on a rigid body hypothesis. This kinematic solver shares the same API than the DeepLines Wind$^{TM}$ solver, ensuring the validity of the coupling.

### 2.5. Calculations setup
In order to ensure the convergence of the results, azimuthal steps of $10°$ per time step for 10 to 15 rotations of the wind turbine have been used. Both AeroDeeP and CASTOR use 30 cosine distributed elements per blade, thus ensuring a good refinement near the root and the tip, and PUMA uses 25 square root distributed elements, ensuring a good refinement near the tip. All solvers share the same airfoil data.

## 3. Experimental data
Experimental data from both the UAE Phase VI experiments and the MexNext project have been used for comparison. For more details about the experiments, see [3] and [13].

### 3.1. Unsteady Aerodynamics Experiment Phase VI
The Unsteady Aerodynamic Experiment (UAE) Phase VI have been carried out in the $24.2 \times 36.6m$ NASA Ames wind tunnel. A $10.1m$ diameter two-bladed wind turbine rotor was used. In the considered cases, the rotor rotates at approximately $72rpm$, the blades are pitched by an angle $\theta = 3°$ for the sequence H considered below, and with a variable pitch for the dynamic inflow Q sequence. The twisted and tapered blades are based on $S809$ airfoils. Both blade coning and hub tilt angles are zeros. Normal and tangential forces distributions are obtained through the integration of the measured pressures at five radial positions along the blades. Normal force is supposed to be positive while pointing from the pressure side to the suction side of the airfoil. Tangential force is positive while pointing from the leading edge towards the trailing edge of the airfoil. Complete description of the wind turbine and available data can be found in [3]. We used the $S809$ airfoil polar data provided in [3] (without corrections for the rotational effects), together with transition airfoils near the root (between the cylinders and the $S809$ airfoils).

### 3.2. MEXICO rotor
The MEXICO and New MEXICO experiments have been performed in the $9.5 \times 9.5m^2$ DNW closed walls large low-speed facility test section, using a $4.5m$ diameter three bladed rotor. In the considered cases, the rotor rotates at approximately $424.5rpm$, and the blades are pitched by an angle of $\theta = -2.3°$. The twisted and tapered blades are based on $DU91$-$W2$-250, $RISO$-$A1$-21 and $NACA64$-418 airfoils from root to tip. Both blade coning and hub tilt angles are zeros. Normal and tangential forces distributions are obtained through the integration of the measured pressures at five radial positions along the blade, using the same sign convention than the UAE experiments. A complete description of the experiment can be found in [13]. Airfoil data have not been corrected for rotational effects. Transition airfoils have been used between the various profiles.

## 4. Axial Inflow
A first comparison for the axial inflow test cases is shown figure 1. The BEM solver and both lifting-line solvers are compared to the Sequence H of the UAE measurements. Forces normal and tangential to the chord line are presented in function of the non-dimensional spanwise location

for three wind velocities: $U_\infty = 5, 7$ and $10m/s$. The spanwise location is non-dimensionalised by the turbine radius (starting from the hub center). Mean experimental values of the normal and tangential forces are used. With the exception of some discrepancies at the blade extremities,
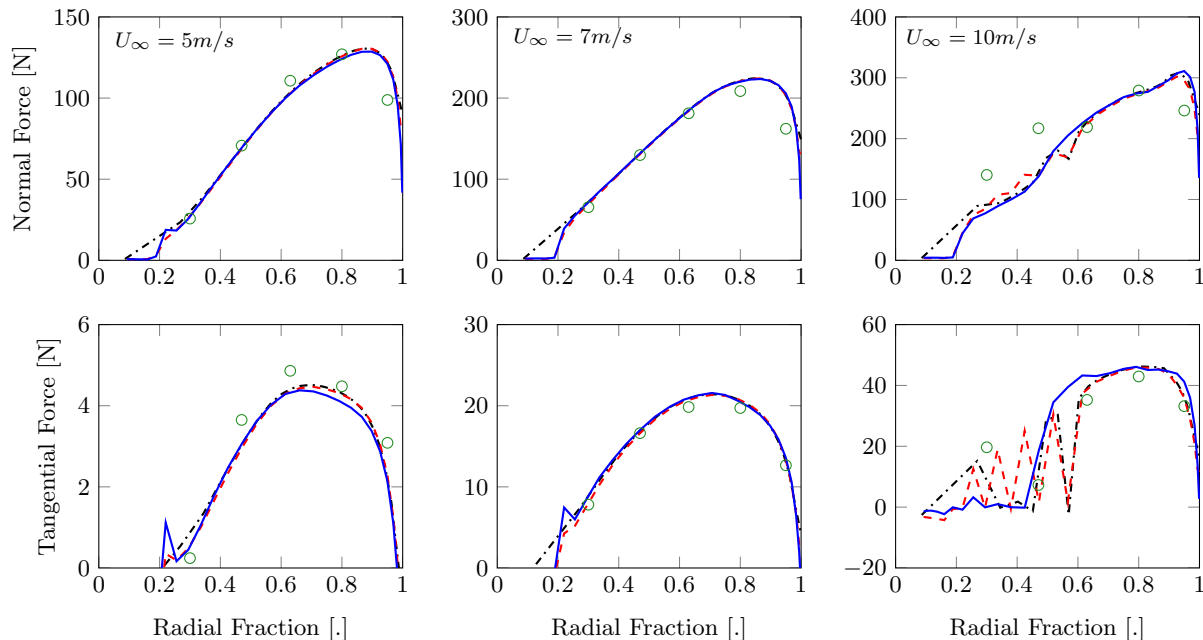


**Figure 1.** UAE Phase VI, Sequence H: wind velocity $5m/s$ (left), $7m/s$ (middle) and $10m/s$ (right). The green circle ○ represent the UAE experiments, the blue line ── the BEM simulations, the red dashed line --- the Lifting-Line (Prandtl) simulations/ and the black dashed line --·- the Lifting-Line (Mudry) simulations.

the three solvers present a very good agreement with the experimental data at 5 and $7m/s$. Even at the tip, BEM results are very close to the lifting-line solvers. It is expected that the discrepancy observed near the root (below 0.25) between the Murdy's lifting line solver and the other solvers can be explained by different blade discretizations (cosine distribution versus square-root distribution). Near the tip ($r/R > 0.85$) the normal force is over-estimated by about 20% by the three solvers, potentially shifting the position of the maximum normal force. Due to the low resolution of the experimental data and the strong gradient of the force near the tip, the exact position of the maximum normal force is not clear, and small deviation can lead to high error percentage. It is then difficult to conclude on the models accuracy regarding the representation of the force evolution. At $5m/s$, a small deviation (below $1N$) is observed on the tangential force at mid-span, but due to the low magnitude of the force (below $5N$) it is hard to conclude if the difference is significant. At $10m/s$, strong discrepancies appear in the range $r/R = [0 - 0.6]$. The few experimental points indicate a strong oscillation of the normal force which is not captured by the BEM solvers. The lifting-line solvers predict strong oscillations, the frequencies of which depending on the model, but due to the lack of experimental data it is not possible to conclude on the accuracy of the models. The oscillations are induced by the presence of a stalled flow, which seems a limitation of the three tested solvers. The wake models seems to have an influence on the stalled flow representation as the two lifting-line models predict oscillations with different frequencies.

A second comparison for the axial inflow test cases is shown figure 2. Each solver is compared to the New MEXICO measurements (using the rough NACA dataset) at three wind velocities:

10, 15 and $24m/s$. A very good agreement between the experimental data and the solvers is
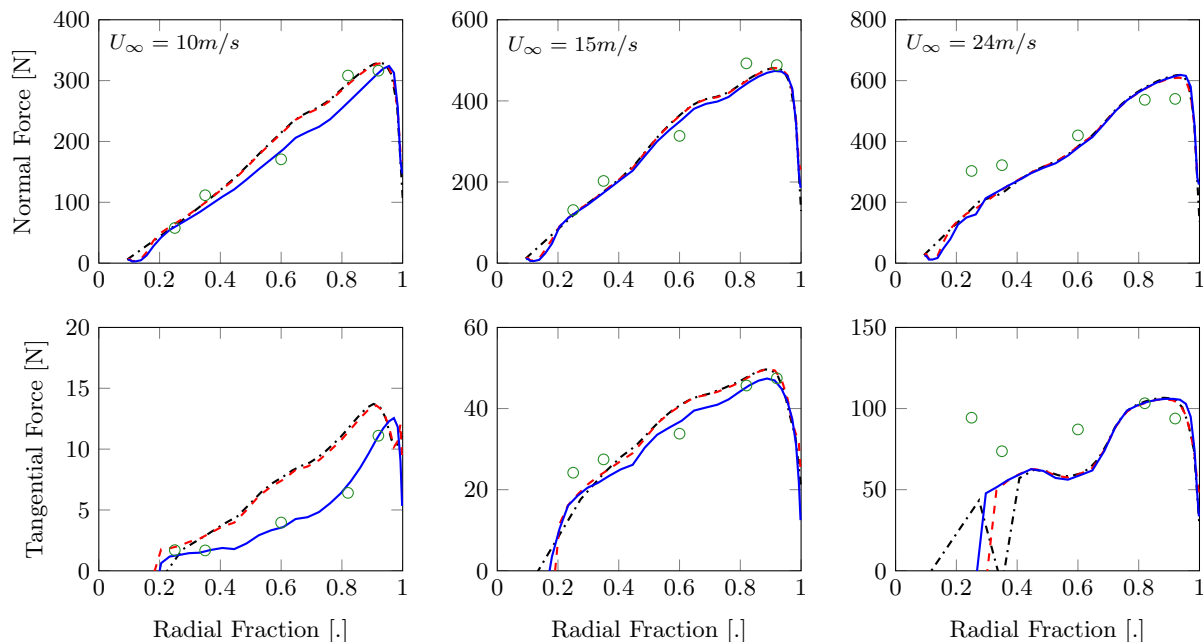


**Figure 2.** New MEXICO: Normal (top) and tangential (bottom) forces along the blade, wind velocity $10m/s$ (left), $15m/s$ (middle) and $24m/s$ (right). ○: UAE experiments / ——: BEM / : Lifting-Line (Prandtl) / ---- : Lifting-Line (Mudry)

observed at 10 and $15m/s$ for the normal force. In the turbulent wake state regime (lower wind velocity, $10m/s$), a strong discrepancy can be observed between the lifting results and the experimental tangential force while the BEM predictions are very close to the experimental results. BEM results are driven by the Glauert correction for high induction in this case, which leads to very good results. The discrepancy between lifting-line solvers and experiments is still under investigation. At high wind velocity (figure 2, right), both normal and tangential forces appear to be slightly over-predicted near the tip of the blade, and under-predicted near the root by all three methods. At this tip speed ratio, the flow is separated from the root to the mid-span of the blade, and some oscillations are observed on the tangential forces. Globally, apart in the stalled flow regions, a very good agreement is observed between the three solvers and the experimental data. For the UAE case, BEM and lifting-line results are almost super-imposed. However, on the New MEXICO case, the BEM model predicted slightly lower values for the normal and tangential component of the forces. At the lower wind speed (in the turbulent wake state regime), BEM results are closer to experiments than the lifting-line results. On those steady cases, the two lifting-line formulations and wake models appear to be strictly equivalent, apart in the stalled flow regions. The stalled flow regime is clearly a limitation of the three approach and would necessitate more investigations.

## 5. Yawed Inflow
The second test cases concern the yawed inflow. To facilitate the results interpretation, both tower-shadow and dynamic stall models have been deactivated: even so dynamic stall is supposed to occur on those test cases (especially near the root of the blade), the difference in the stall models used in the three solver could complicate the solver comparison. Normal and tangential

forces as a function of azimuth angle are compared to experimental data at three radial positions: $r/R = 0.30$, $r/R = 0.63$, $r/R = 0.95$ for the UAE experiments, $r/R = 0.25$, $r/R = 0.60$, $r/R = 0.92$ for the MEXICO experiments. As predicted by the axial inflow results, an over-estimation of the normal force amplitude (around 20%) is expected with the three solvers at position $r/R = 0.95$ for the UAE experiments and at both $r/R = 0.60$ and $r/R = 0.92$ on the normal and tangential forces for the MEXICO experiments. The force will then be compared in term of variations over the azimuth rather than in term of absolute values. More specifically, we will focus on the ability of the solvers to capture the phase lag on the normal loads between the tip and the root of the blade. As explained in [11], near the tip, the maximum of the normal force is supposed to be located in the upwind part (azimuth range $[180° − 360°]$, the blade is located in an upwind position with respect to the non-yawed configuration), whereas near the root, the maximum is located in the downwind part (azimuth range $[0° − 180°]$). This phase shift, which is due to the presence of the tip and root vortices, leads to a destabilizing yawing moment at the root and a stabilizing yawing moment at the tip [11]. Sequence H of the UAE experiments is used again. Based on the axial inflow results, we use a wind velocity of $7m/s$, at which the best agreement between calculations and experiments was observed (figure 1). Experimental data presented in the following figures have been filtered using Legendre polynomials. The first case corresponds to a yaw angle $\Psi = 20°$ (figure 3). Near the blade root
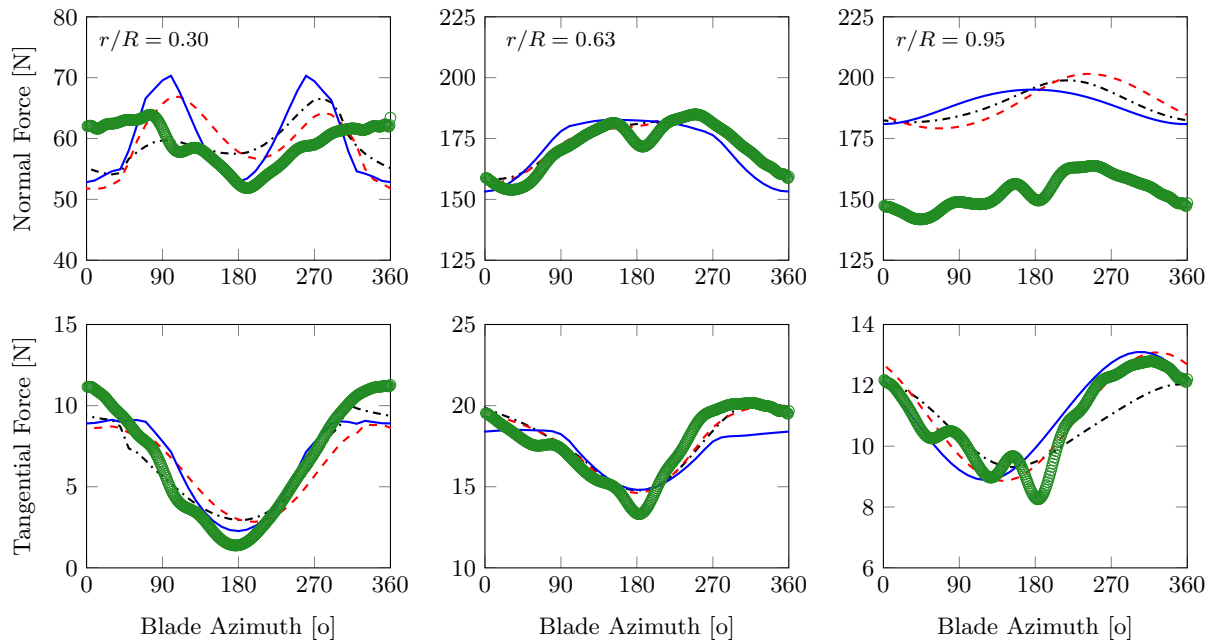


**Figure 3.** UAE Sequence H: Normal (top) and tangential (bottom) blade loads evolution with azimuth at radial fraction 0.30, 0.63, 0.95, wind velocity $7m/s$, yaw angle 20°. ◯: UAE experiments / ——: BEM / - - - -: Lifting-Line (Prandtl) / —·—·: Lifting-Line (Mudry)

$(r/R = 0.30)$, the shape of the tangential forces fluctuations is quite well reproduced by the three solvers with a slight underestimation of the variation amplitude. For the normal forces, a strong discrepancy can be observed between the simulations and the experimental results, with an over-estimation of the maximal amplitude of the fluctuations around azimuth 90 and 270°. All three solvers predict a strong decrease of the normal force around azimuth 0 and 360° which is not observed experimentally. Further investigations have shown than the dynamic stall phenomena plays an important role here. A strong discrepancy between the solvers is also

observed. At mid-span ($r/R = 0.63$), both the amplitude of the fluctuations and the mean value of the normal and tangential forces are close to the experiments for the three solvers. The BEM solver fails to predict the phase shift, thus over-estimating the normal forces in the downwind part and underestimating them in the upwind part. Near the tip, the normal force is over-estimated in average, as expected (figure 1). The lifting-line solvers predict the shape of the fluctuations and the phase shift accurately, while the BEM solver has a symmetric behaviour, predicting the maximal normal force around azimuth 180° rather than 250°. Discrepancies are observed between the Prandtl and the Mudry lifting-line solvers, for both the normal and the tangential forces: the phase shift and the amplitude of the fluctuations are better predicted with the Prandtl solver. The disabling of the tower shadow model could explain the disregard of the small kink observed around azimuth $\Phi = 180°$ at mid-span and near the tip. This point deserves further investigations.

For the second case, an higher yaw angle ($\Psi = 60°$, figure 4) has been chosen. Near the
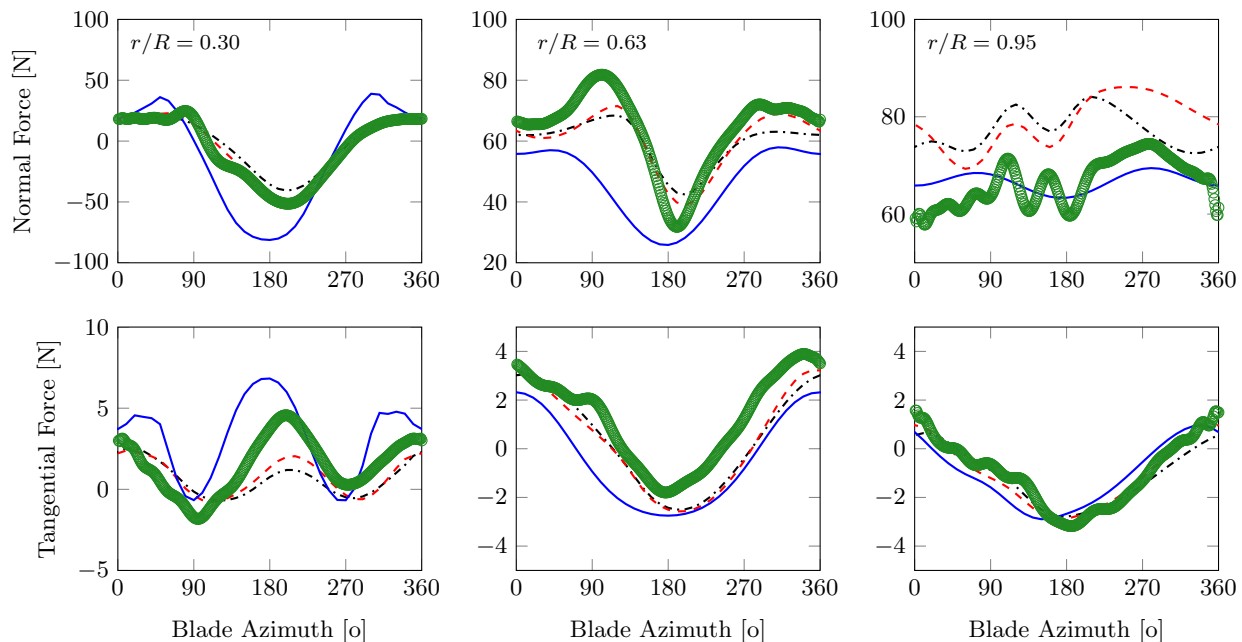


**Figure 4.** UAE Sequence H: Normal (top) and tangential (bottom) blade loads evolution with azimuth at radial fraction 0.30, 0.63, 0.95, wind velocity $7m/s$, yaw angle 60°. ◯: UAE experiments / ——: BEM / ----: Lifting-Line (Prandtl) / ---: Lifting-Line (Mudry)

root, the BEM solver largely over-predicts the tangential force fluctuations, whereas the lifting-line solvers tend to under-predict them. A phase-lag of 50° can also be noticed between the BEM prediction of maximal tangential force and the experimental results, whereas the lifting line solvers predicted it accurately. The lifting-line solvers predictions of the normal force are very good, while similarly to the $\Psi = 20°$ case, the BEM model largely over-estimates the fluctuations magnitudes. At mid-span, the lifting-line solvers do predict the normal loads evolution accurately, despite a small under-prediction of the load amplitude. The BEM solver increases this error. Near the tip of the blade, normal forces fluctuations are rather small in amplitude, and thus difficult to interpret. However, the Mudry's lifting-line model does not predicts the augmentation of the normal force in the upwind part accurately, contrary to the Prandtl solver. On the tangential loads, despite a very good agreement, a small phase lag can be observed between the BEM predictions and the experimental results. Globally, the Prandtl

lifting-line solver is able to reproduce the phase shift in the normal forces accurately. The Mudry's lifting-line solver behaves pretty well in the downwind part, but some discrepancies have been observed in the upwind part. The results of the BEM model are less accurate than the lifting-line ones, but do follow the main experimental trends. This is due to the complex flow field in yaw: while rotating, each blade experiences an advancing and retreating motion, inducing sinusoidal variations of relative velocities, which are well caught by BEM and lifting-line solvers. However, the BEM theory does not model the tip and root vortices, and thus cannot predict the phase shift phenomena. Those observation are confirmed by the results obtained with the MEXICO dataset, one which the phase shift phenomena is also clearly visible (figure 5). A comparison has been made between experimental results and simulations for a 30° yaw angle and a wind velocity of $15m/s$.
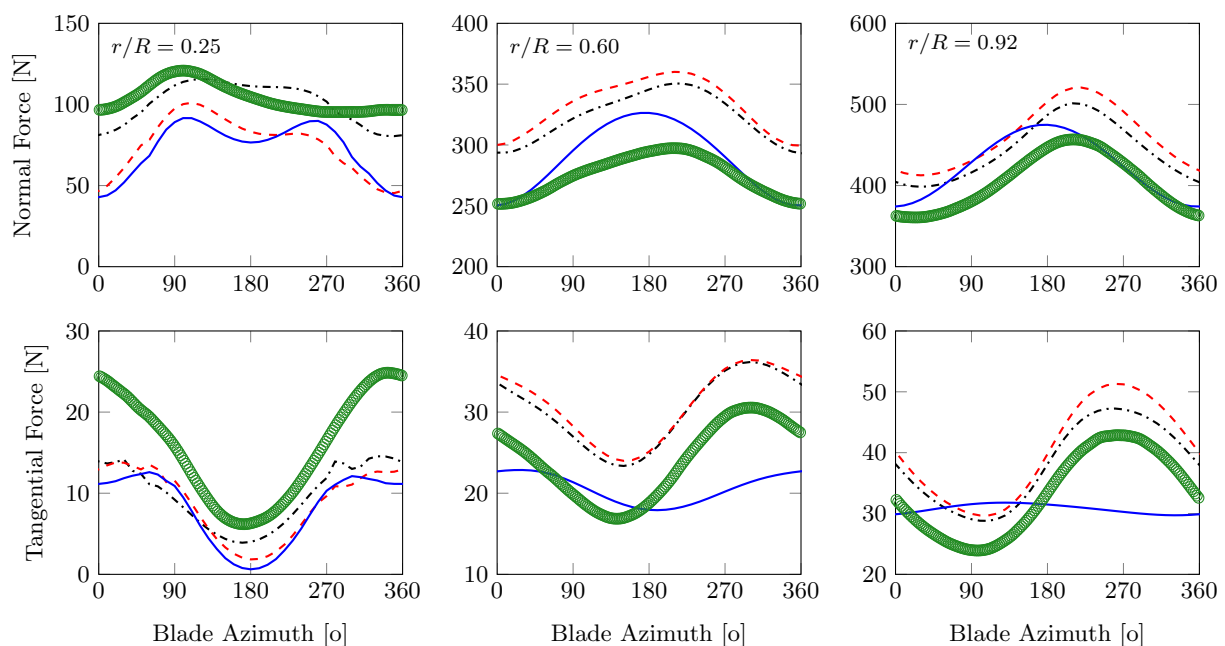


**Figure 5.** MEXICO: Normal (top) and tangential (bottom) blade loads evolution with azimuth at radial fraction 0.25, 0.60, 0.92, wind velocity $15m/s$, yaw angle 30°. ○: MEXICO experiments / ——: BEM / - - - : Lifting-Line (Prandtl) / -·-·- : Lifting-Line (Mudry)

Near the root of the blade, the maximum of the normal force is located near the azimuth 90°, in the downwind part. This is well predicted by the lifting-line solvers, but they also predict a smaller second pic around 270°, which, following the previous analysis, should be attributed to an over-estimation of the strength of the tip vortex in the downwind part. Due to the absence of tip and root vortices, the BEM model has an unrealistic symmetric behaviour. Compared to the Murdy approach, the Prandtl solver underestimate the normal load amplitude by $50N$. This is one of the few configuration where a strong difference in amplitude can be observed between the two lifting-line solvers. At this spanwise location, the tangential force variations are underestimated by all three solvers. Around mid-span, the maximum of the normal force is located in the upwind part of the blade (azimuth $\Phi = 210°$). The two lifting line solvers predict the amplitude of the fluctuations and the phase shift accurately, despite an over-prediction (around 20%) of the mean value, which was expected (figure 2). In contrast, the BEM under-predicts the amplitude of the fluctuations of the tangential loads and over-predicts those of the normal loads, but the mean values of the forces are more accurately predicted. Similar

observations can be made near the tip. As a conclusion for the yawed inflow cases, it can be said that lifting-line solvers do reproduce the measured load fluctuations very well, predicting the phase shift accurately, which was expected (see [11], [5]). Differences have been observed in the upwind part between the two lifting-line solvers, but only on the UAE test cases where the Prandtl lifting-line solver appears to be more accurate. The BEM model provides a good representation of the load fluctuations, due to the valid representation of the advancing and retreating motion of the blades, but neglects the phase shift, which is due to the interactions between the blade and the tip/root vortices, thus missing a large part of the ongoing physics in yawed cases. This phase shift induces a varying yawing moment that may increase the blade fatigue, and is thus of major importance for the design. For the yawed cases, lifting-line solvers appear more reliable than the BEM solver. Further investigations including dynamic stall models are ongoing.

## 6. Dynamic Inflow

The last comparison concerns the dynamic inflow phenomena. The UAE Phase VI sequence Q data are used here. The simulations have been performed using the BEM solver, with the Øye dynamic inflow correction activated, and with the Prandtl lifting-line model. Due to numerical robustness issues, we have not been able to reproduce this case with the solver based on Mudry's theory. Both rotational velocity and pitch angle time series issued from measurements have been imposed as an input condition to the solvers. Two wind velocities are considered (5 and $10m/s$). Similar results have been observed for a wind velocity of $8m/s$. At $5m/s$, the blade tip pitch
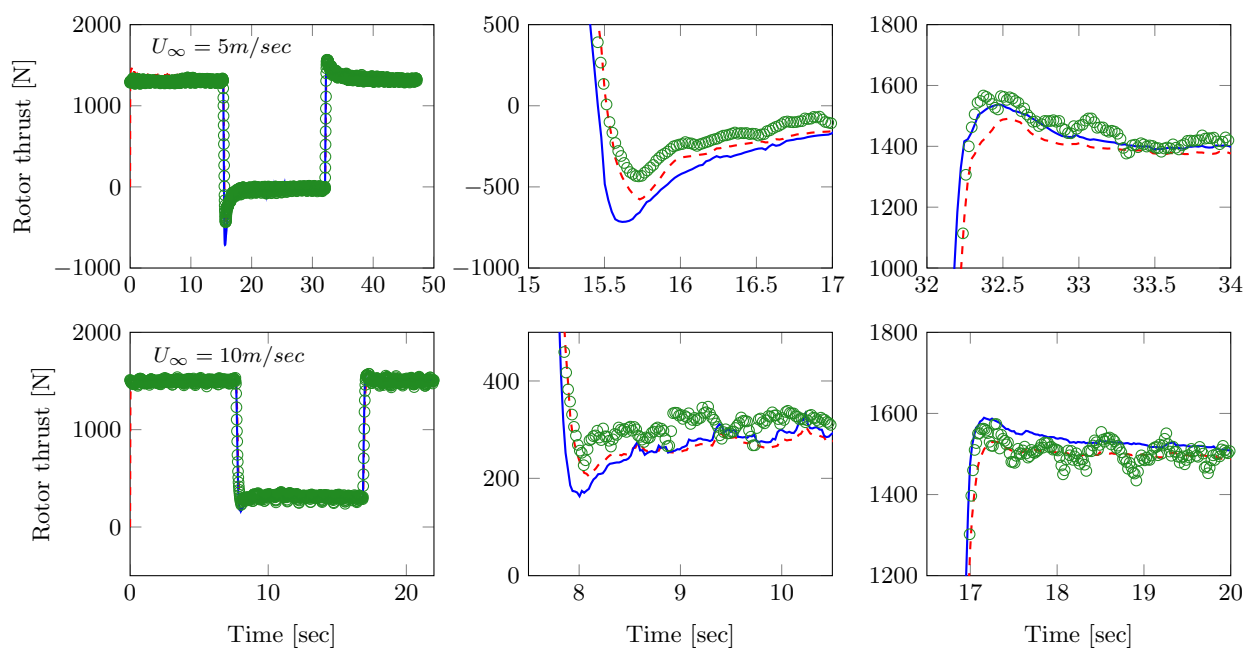


**Figure 6.** UAE Phase VI: Rotor thrust evolution during pitch steps (left) and close-ups (center and right), wind velocity = $5m/s$ (top) and = $10m/s$ (bottom). ◯: UAE experiments / ——: BEM / - - - : Lifting-Line (Prandtl)

varies from $-6$ to $+10$ degrees every 15 seconds, with a pitch rate of $66deg/s$. For the $10m/s$ test cases, the blade tip pitch varies from $+6$ to $+24$ degrees every 8 seconds, with a pitch rate of $66deg/s$. With both BEM and lifting-line solvers, an excellent agreement is observed between

measurements and calculations. Despite the small offset on the total rotor thrust, the overshoot on the thrust for both the upward (figure 6, center) and downward (figure 6, right) facing steps is pretty well caught. This test case highlights the capability of the corrected BEM and lifting-line solvers to handle unsteady flows, even if the time scales encountered in such kind of tests are by order of magnitude larger than the one due to standard blade pitch control or wind turbine floater motions.

## 7. Conclusion

Three different solvers have been compared and validated: a first solver based on the Blade Element Momentum theory, a second based on the Prandtl lifting-line theory, and a third one based on the more recent Mudry's theory. Those solvers are intended to be coupled with the aero-servo-hydro-elastic solver DeepLines Wind$^{\text{TM}}$, in order to simulate fully coupled floating offshore wind turbine systems. In the present framework, we used a rigid body hypothesis in order to get more insight into aerodynamic phenomena. Two sets of experimental data have been used, the UAE experiments and the MEXICO / New MEXICO experiments. For the axial flow cases, all three solvers compare very well against the experiments, and very similar results were obtained. In yawed conditions, lifting-line solvers behave very well and are able to catch some relatively fine phenomenon dealing with the tip and root vortices and leading to a dephasing in the location of the maximum normal force between the tip and the root of the blade. The BEM solver, which was globally in good accordance with the experimental data, is not able to catch this phenomenon, leading to a possible inacurate prediction of the global yawing moment of the wind turbine. This could be disqualifying when dealing with full floating wind turbine systems. Last, the BEM and Prandtl lifting-line solvers results have been compared to experimental data on unsteady cases, on which turbine blades were pitched sharply. Both the BEM and the Prandtl lifting-line solver behave very well, which underlines the ability of the unsteady BEM theory to handle the various types of unsteadiness involved in FOWT simulations, even so such test cases are not necessarily representative of the time scales of the unsteady phenomena present in FOWT standard operations.

## References

[1] E. Branlard, M. Gaunaa, Development of new tip-loss corrections based on vortex theory and vortex methods, Proceedings of the TORQUE 2012 conference, The Science of Making Torque from Wind, 2012.
[2] T. Chaviaropoulos, H.-J. Kooijman, J. Madsen, G. Schepers, N. Sorensen, M. Stettner, AVATAR Deliverable D1.1 Reference Blade Specification, AVATAR project deliverable, 2014.
[3] H. Hand, D. Simms, L. Fingersh, D. Jager, J. Cotrell, S. Schreck, S. Larwood, Unsteady Aerodynamics Experiment Phase VI: Wind Tunnel Test Configurations and Available Data Campaigns, NREL/TP-500-29955, December 2001.
[4] H. Glauert, Airplane Propellers, Springer Berlin, 1935.
[5] F. Grasso, A. Van Garrel, G. Schepers. Development and validation of Generalized Lifting Line code for Wind Turbine Aerodynamics, Technical Report ECN-M-11-004, ECN, 2011.
[6] M.H. Hansen, M. Gaunaa, H. Aagaard Madsen, A Beddoes-Leishman type Dynamic Stall model in State-Space and Indicial Formulations, Denmark. Forskningscenter Risoe. Risoe-R, No. 1354, 2004.
[7] J. Katz, A. Plotkin, Low-Speed Aerodynamics, 2nd ed. Cambridge: Cambridge University Press, 2001.
[8] C. Le Cunff, J.M. Heurtier, L. Piriou, C. Berhault, T. Perdrizet, D. Teixeira, G. Ferrer, J.C. Gilloteaux, Fully

Coupled Floating Wind Turbine Simulator Based on Nonlinear Finite Element Method: Part I-Methodology, ASME 2013 32nd International Conference on Ocean, Offshore and Arctic Engineering, Vol. 8.

[9] M. Mudry, La Théorie Générale des Nappes et Filaments Tourbillonnaires et ses Applications à l'Aérodynamique Instationnaire, PhD Thesis Université Paris VI, 1982.

[10] A. Robertson et al., Offshore Code Comparion Collaboration Continuation Within IAE Wind Task 30: Phase II Results Regarding a Floating Semisubmersible Wind System (Preprint), 33rd International Conference on Ocean, Offshore and Arctic Engineering, San Francisco, California, NREL/CP-5000-61154, 2014.

[11] J. Schepers, Annexlyse: Validation of Yaw Models, on Basis of Detailed Aerodynamic Measurements on Wind Turbine Blades, ECN-C-04-97.

[12] J. Schepers, Engineering Models in Wind Energy Aerodynamics, Development, Implementation and Analysis using Dedicated Aerodynamic Measurements, PhD Thesis, TU Delft, Netherlands.

[13] H. Snel, J. Schepers, B. Montgomerie, The MEXICO project (Model Experiments in Controlled Conditions): The Database and First Results of Data Processing and Interpretation, The Science of Making Torque from Wind Conference, Journal of Physics: Conference Series 75, 2007.

[14] J. Weissinger, The Lift Distribution of Swept-Back Wings, NACA Technical Memorandum N. 1120, 1947.